Performance analysis in multi-hop radio networks with balanced fair resource sharing

Aleksi Penttinen

Helsinki University of Technology (TKK)

Networking Laboratory

P.O. Box 3000

FIN-02015 TKK, Finland

aleksi.penttinen@tkk.fi

Jorma Virtamo

Helsinki University of Technology (TKK)

Networking Laboratory

P.O. Box 3000

FIN-02015 TKK, Finland

jorma.virtamo@tkk.fi

Riku Jäntti

University of Vaasa

Department of Computer Science

P.O. Box 700

65101 Vaasa, Finland

riku.jantti@uwasa.fi

Abstract: Balanced fairness is a new resource sharing concept recently introduced by Bonald and Proutière. We extend the use of this notion to wireless multi-hop networks, e.g. ad hoc networks, where the link capacities at the flow level are not fixed but depend on lower layer issues such as scheduling and interference. Utilizing this extension we present the theoretical framework for flow level performance analysis of elastic traffic in the setting, assuming that the wireless bandwidth resources are subject to linear constraints. We discuss how different physical and access layer configurations can be described by the linear constraint model and devise an efficient computational scheme for solving the system. The concepts and the computational scheme are illustrated by a number of examples.

Keywords: Wireless multi-hop networks, flow-level performance evaluation, balanced fairness

Submitted: November 19th 2004

Revised: November 9th 2005

1 Introduction

As in fixed networks, also in wireless multi-hop networks the performance perceived by the users sending elastic traffic mainly manifests itself on the flow level. A flow of elastic traffic typically comprises of a transfer of a document, file or message. The transmission can use all the bandwidth that is available but can also adapt the transmission speed to share the bandwidth with other concurrent flows. The performance, measured for instance in terms of the average transfer time of a document of a given size, clearly depends on the dynamic behavior of the system and on how the bandwidth is shared between different flows. Thus it is necessary to study the system in a dynamic setting where new flows arrive at the network, are transferred across the network, and upon completion depart from the system.

This problem has been recently addressed in the context of fixed networks (Bonald and Proutière (2004, 2003); Bonald et al. (2003)). However, the flow level performance of multi-hop radio networks, or ad hoc networks, is considerably more intricate because of the complex interactions pertaining to the shared RF channel and its use. This was realized already in the early work on general analytical modeling of packet radio networks by Tobagi (1987). As far as we are aware, paper Penttinen and Virtamo (2004) by the present authors was the first analysis of this type for static ad hoc networks. The current article expands and generalizes our earlier work.

Fairness of the bandwidth sharing has been recognized as an important consideration in the context of fixed networks. Several fairness concepts have been introduced and analyzed, cf. Mo and Walrand (2000); Massoulié and Roberts (2002). In ad hoc networks fair bandwidth sharing has been studied in Tassiulas and Sarkar (2002), Huang and Bensaou (2001) and Luo et al. (2000), where the authors have presented centralized and distributed algorithms that can be used to allocate max-min fair rates for a given set of flows under some specific network models. Although the allocation could be made optimal in the sense of a utility function for any given fixed set of flows, it does not necessarily guarantee that

the system converges to a steady state that is optimal in the dynamic scenario (Bonald and Proutière (2003)). Also, an analysis of the performance of max-min fair resource sharing in a dynamic setting would be prohibitively difficult.

A new concept of balanced fairness (BF) has recently been introduced by Bonald and Proutière (2002, 2004). This is a very interesting notion on two accounts. First, it leads to a network performance which does not depend on the traffic characteristics except the traffic intensity on the different paths, in other words, the performance under BF is insensitive. Secondly, for simple systems BF often allows an explicit analysis of the performance in the dynamic setting.

Simulation studies of fixed networks have shown that in many cases the performance of a network under BF is similar to that under max-min fairness (Bonald and Proutière (2003); Timonen (2003)). BF provides therefore a useful approximation tool for evaluating network performance. However, BF itself does not represent a solution to a utility optimization problem or guarantee Pareto efficient use of the resources.

In this article we introduce a natural extension of the notion of balanced fairness to take into account the fact that in a wireless multihop network the capacities of the links can be changed by the lower layer parameters. In other words, capacity can be shifted from one part of the network to another within certain limits. The resulting BF resource sharing problem is a joint problem of determining both the state-dependent lower layer parameter configuration and bandwidth allocation to maximize the use of the network resources, while at the same time retaining the balance and the related insensitivity properties. To solve the problem in a general resource model, an efficient computational method is devised. These contributions enable insensitive performance analysis of wireless ad hoc networks.

This paper is organized as follows. Section 2 presents the key theoretical concepts and presents the framework of flow level performance analysis of wireless ad hoc networks. In Section 3 we show how the resource model used in the analysis can be tailored to conform to different physical and access layer models. Section 4 describes an efficient computational

algorithm for the analysis and Section 5 contains the examples which illustrate various aspects of the approach. We conclude finally in Section 6.

2 Theoretical framework

In this section we review the concept of balanced fairness and present how it can be extended to wireless multi-hop networks. Furthermore, we outline our resource model to describe wireless network capacity and integrate the model with the balanced fairness resource sharing.

2.1 Extension of Balanced Fairness

Consider a static network consisting of J unidirectional links and carrying N classes of elastic flows using pre-defined routes. Let $\mathbf{A}$ be the incidence matrix denoting the set of flows using the links such that $a_{ji} = 1$ if flow class i uses the link j, else $a_{ji} = 0$. We also denote by $\mathcal{F}_j = \{i : a_{ji} = 1\}$ the set of flows using link j.

The network state is represented by the vector $\mathbf{x} = (x_1, \ldots, x_N)$ in which x_i is the number of class-i flows in progress. Let $\phi_i(\mathbf{x})$ be the bandwidth allocation to class i in state $\mathbf{x}$, which is equally shared by all flows of class i. An allocation is said to be balanced if it holds that

$$\frac{\phi_i(\mathbf{x} - \mathbf{e}_j)}{\phi_i(\mathbf{x})} = \frac{\phi_j(\mathbf{x} - \mathbf{e}_i)}{\phi_j(\mathbf{x})} \qquad \forall i, j,\ x_i > 0,\ x_j > 0 \ ,$$

where $\mathbf{e}_i$ is an N-vector with 1 in the ith component and 0 elsewhere. Bonald and Proutière (2002) show that an allocation is balanced if and only if the allocations can be expressed in terms of a so-called balance function $\Phi(\mathbf{x})$ as

$$\phi_i(\mathbf{x}) = k\ \Phi(\mathbf{x} - \mathbf{e}_i) \ , \tag{1}$$

where the proportionality constant is $k = 1/\Phi(\mathbf{x})$. Conversely, any positive function $\Phi(\mathbf{x})$ defines a balanced allocation by (1).

Balanced fairness as defined by Bonald and Proutière (2002, 2004) refers to the most efficient balanced allocation in the sense that in each state of the system at least one of the links is saturated. This leads to a unique allocation: denoting the capacity of link j by c_j, the balance function is uniquely defined by the recursion,

$$\Phi(\mathbf{x}) = \max_j \frac{1}{c_j} \sum_{i \in \mathcal{F}_j} \Phi(\mathbf{x} - \mathbf{e}_i) \;=\; \max_j \frac{b_j(\mathbf{x})}{c_j} \;, \tag{2}$$

with $\mathbf{b}(\mathbf{x}) = \mathbf{A}\tilde{\mathbf{\Phi}}(\boldsymbol{x})$, where $\tilde{\mathbf{\Phi}}(\boldsymbol{x}) = (\Phi(\mathbf{x} - \mathbf{e}_1), ..., \Phi(\mathbf{x} - \mathbf{e}_n))^{\mathrm{T}}$. The seed of the recursion can be arbitrarily set, e.g. $\Phi(\mathbf{0}) = 1$.

The extended balanced fairness principle just says that, in each state $\mathbf{x}$, the proportionality constant $k = 1/\Phi(\mathbf{x})$ is chosen as large as allowed by whatever constraints the system is subject to. In the case of fixed routes and fixed link capacities this leads to (2).

In the case of multi-hop radio networks, we assume that we have fixed routes but the link capacities $c_j(\upsilon)$ relate to a virtual network $\upsilon \in \Upsilon$, which is a flow level abstraction of the average bit pipes that the network can support. This additional degree of freedom arises from the lower layer configurations such as coding, modulation, power control and scheduling. We will return to the modeling aspects in more detail in Section 3. In the extended model the balance function $\Phi(\mathbf{x}) = 1/k$ of BF is now simply determined by the recursion

$$\Phi(\mathbf{x}) = \min_{\upsilon \in \Upsilon} \max_j \frac{1}{c_j(\upsilon)} \sum_{i \in \mathcal{F}_j} \Phi(\mathbf{x} - \mathbf{e}_i) \;=\; \min_{\upsilon \in \Upsilon} \max_j \frac{b_j(\mathbf{x})}{c_j(\upsilon)} \;. \tag{3}$$

For each state $\mathbf{x}$, this recursion defines both the balance function $\Phi(\mathbf{x})$ and the virtual network $\upsilon = \upsilon(\mathbf{x})$.

Assume that the flow durations are long compared with the time scale of changing the virtual network, e.g. the time it takes for the protocol or flow control mechanism used for the bandwidth sharing to find a steady state. Thus we assume that as soon as a flow arrives or departs, a new steady state, with a new virtual network and its resource sharing, is reached

instantaneously.

We make the assumption on the arrival process that the flows are generated by sessions (see Bonald and Proutière (2004, 2003)), each session being composed of a random number of flows separated by think times. Flow sizes and think time durations can be arbitrarily distributed and need not to be independent. If balanced resource allocation is used and the sessions arrive as a Poisson process then, as shown in Bonald and Proutière (2004, 2003), the steady state distribution of the network state is given by

$$\pi(x_1, \ldots, x_N) = \frac{1}{G(\boldsymbol{\rho})} \Phi(x_1, \ldots, x_N) \rho_1^{x_1} \ldots \rho_N^{x_N} \quad , \tag{4}$$

and depends on the traffic characteristics only through the traffic loads ρ_i of different routes. Load ρ_i is the product of the flow arrival rate and mean flow size on route i.

In (4), $G(\boldsymbol{\rho})$ is the normalization constant

$$G(\boldsymbol{\rho}) = \sum_{x_1=0}^{\infty} \cdots \sum_{x_N=0}^{\infty} \Phi(x_1, \ldots, x_N) \rho_1^{x_1} \ldots \rho_N^{x_N} \quad , \tag{5}$$

which depends on the traffic load vector $\boldsymbol{\rho} = (\rho_1, \ldots, \rho_N)$. The normalization constant $G(\boldsymbol{\rho})$ is an important quantity as the performance measures can be derived from it. Under a specific condition detailed in Bonald et al. (2003) the constant can be calculated recursively directly without even solving $\Phi(\mathbf{x})$. In the first example presented later in this paper (Ex. 1, Sect. 5) the condition is satisfied and the normalization constant can indeed be obtained in a simple way. In general, one must resort to numerical analysis and evaluate the state probabilities (4) for a sufficient number of states to approximate the state distribution for any given traffic load vector $\boldsymbol{\rho} = (\rho_1, ..., \rho_N)$ with an arbitrary accuracy.

A key performance measure for class-i flows is the throughput γ_i, defined as the ratio of the mean flow size to the mean flow duration. By Little's result this is equal to $\rho_i / \mathrm{E}[x_i]$.

The denominator can be obtained by derivation yielding

$$\gamma_i = \frac{G(\boldsymbol{\rho})}{\frac{\partial}{\partial \rho_i} G(\boldsymbol{\rho})} \ . \tag{6}$$

We reiterate that balanced fairness has the very desirable property that the performance of the network is *insensitive* to traffic details. Furthermore, it allows us to evaluate the performance by (3), (5) and (6).

2.2 General form of the recursion

Here we elaborate equation (3) in the case that the resources, the capacities of virtual networks, are subject to linear constraints. The model corresponds to scheduling of different transmission parameters throughout the network.

2.2.1 Wireless network resource model

At any instant, the network operates in a single transmission mode $\tau \in \mathcal{T}$, which defines the controllable communication parameters uniquely at the physical and access layers for each link. For instance, τ may define which links are active or what modulation schemes and transmission powers are used. At this short time scale, the links of the network can be seen as fixed bit pipes, the capacities of which arise from the parameters defined by the mode. The set of all transmission modes $\mathcal{T}$ is the set of all the possible combinations of the lower layer parameters on the links.

Each transmission mode defines the capacities of the simultaneously sustainable bit pipes in the network, $\mathbf{v}(\tau) = (v_1(\tau), \ldots, v_J(\tau))^{\mathrm{T}}$. We define the set of instantaneous rate vectors to contain all feasible capacity combinations, including those in which all the available capacity is not used (or used by "virtual" traffic), i.e. $\mathcal{R} = \{\mathbf{r} = (r_1, \ldots, r_J)^{\mathrm{T}} \mid \mathbf{0} \leq \mathbf{r} \leq \mathbf{v}(\tau),\ \tau \in \mathcal{T}\}$.

As the flow level virtual networks operate at an essentially longer time scale, also all the rates obtained by time multiplexing the vectors in $\mathcal{R}$ are available to flows. Hence we define

the set of virtual networks Υ in the flow level abstraction as the convex hull of $\mathcal{R}$. Formally, the convex hull is defined as

$$H(\mathcal{R}) = \{\mathbf{r} \,|\, \mathbf{r} = \mathbf{R}\mathbf{p},\, \mathbf{e}^{\mathrm{T}}\mathbf{p} \leq 1,\, \mathbf{p} \geq \mathbf{0}\} \ , \tag{7}$$

where $\mathbf{e} = (1, 1, ..., 1)^{\mathrm{T}}$. Matrix $\mathbf{R} = (\mathbf{r}_1, ...)$ is constructed from the extremal rate vectors $\mathbf{r} \in \mathcal{R}$ that are active in spanning the hull (not including the zero vector), i.e. from the vectors that cannot be expressed as convex combinations of any other vectors of the hull. The parameter $\mathbf{p}$ can be interpreted as the schedule with each component p_i being the fraction of time rate vector i is used.

2.2.2 Integrating the resource model with balanced fairness

Using the resource model defined above, we can write the balance function as

$$\Phi(\mathbf{x}) = \min_{\mathbf{r} \in H(\mathcal{R})} \max_j \frac{b_j(\mathbf{x})}{r_j} \ . \tag{8}$$

The terms

$$b_j(\mathbf{x}) = (\mathbf{A}\tilde{\mathbf{\Phi}}(\mathbf{x}))_j = \sum_{i \in \mathcal{F}_j} \Phi(\mathbf{x} - \mathbf{e}_i) \tag{9}$$

determine the proportions of resource demands set on each link j in state $\mathbf{x}$. The recursion step corresponds thus to finding the virtual network which has the largest feasible rate vector $\mathbf{r}$ with the given proportions, i.e. finding the longest vector in $H(\mathcal{R})$ in the direction of $\mathbf{b}(\mathbf{x})$.

Due to coordinate convexity[1] of the convex hull $H(\mathcal{R})$ (see Appendix A for details on

[1] Coordinate convexity means that if we take any vector from the convex hull and replace any number of its components by zero, the resulting vector still belongs to the hull $\{\mathbf{R}\mathbf{p} \mid \mathbf{e}^{\mathrm{T}}\mathbf{p} \leq 1,\, \mathbf{p} \geq \mathbf{0}\}$.

the equality in the constraints), the recursion step can be written as the LP-problem

$$\begin{aligned} \Phi(\mathbf{x})^{-1} &= \max k \ , \\ \mathbf{R}\mathbf{p} &= k\mathbf{b}(\mathbf{x}) \ , \\ \mathbf{e}^{\mathrm{T}}\mathbf{p} &= 1 \ , \\ \mathbf{p} &\geq \mathbf{0} \ . \end{aligned} \tag{10}$$

By dividing the constraints by k and changing the variable as $\mathbf{p}/k \rightarrow \mathbf{q}$, we get rid of the parameter k and can write the problem more compactly

$$\begin{aligned} \Phi(\mathbf{x}) &= \min_{\mathbf{q}} \mathbf{e}^{\mathrm{T}}\mathbf{q} \ , \\ \mathbf{R}\mathbf{q} &= \mathbf{b}(\mathbf{x}) \ , \\ \mathbf{q} &\geq \mathbf{0} \ . \end{aligned} \tag{11}$$

Each component of the vector $\mathbf{q}$ represents here the duration an extremal rate vector (a given transmission mode) is used. One may imagine the vector $\mathbf{b}(\mathbf{x})$ in the space spanned by the link capacities and the LP-problem is now to express $\mathbf{b}(\mathbf{x})$ with the help of rate vectors $\mathbf{R}$ using the minimal total time.

In the appendix we give a condition on the spanning rate vectors that guarantees that the resulting allocation is Pareto efficient so that no link may contain free capacity. However, this property is not very general; it does not hold even for the case of fixed networks.

2.2.3 Alternative formulation for the recursion

Equivalently, one can define the convex hull of available rates, $H(\mathcal{R})$, as an intersection of half-spaces defined by the constraining hyperplanes (one for each facet) in the form

$$\mathbf{D}\mathbf{r} \leq \mathbf{d} \ . \tag{12}$$

Matrix $\mathbf{D}$ and vector $\mathbf{d}$ can be determined from $\mathbf{R}$, though generally this process is laborious. However, in some cases the constraints are easily available, cf. Example 1 in Section 5.

Now the link rates have explicit constraints and we need not find out the schedule. In this case, the recursion (8) can be replaced with relation

$$\Phi(\mathbf{x}) = \max_i \left\{ \frac{1}{d_i} \left(\mathbf{D}\mathbf{b}(\mathbf{x}) \right)_i \right\} \quad . \tag{13}$$

Note that the only restriction on modeling of physical or link layers in the convex hull model is that the constraints on link rates have to be linear. In fixed networks, matrix $\mathbf{D}$ is the identity matrix and vector $\mathbf{d}$ is the link rate vector, and the above equation reduces to (2).

3 Modeling of ad hoc networks

In the linear constraint model, $\mathbf{R}$ contains all the information of the lower layer configurations. Hence, the modeling process comes down to determining the set of instantaneous rate vectors $\mathcal{R}$. Generally, one selects the set of lower layer parameters to be included in the model and then enumerates the set of feasible parameter configurations and the associated rate vectors.

Ideally, $\mathbf{R}$ contains only the spanning vectors of $\mathcal{R}$, but any additional non-spanning vector in $\mathbf{R}$ is automatically excluded from the optimal solutions (see Appendix B) and is merely a minor computational inconvenience. Next we give examples of the rate vector generation in some common models for wireless networks.

3.1 Effects of transmission power

Assume that the link capacities are based on signal-to-interference ratios (SIR) at the nodes. Let g_{ij} denote the power gain between links i and j, that is the power gain between trans-

mitter of link j and receiver of link i. SIR is defined as

$$s_i = \frac{g_{ii}P_i}{\sum_{j\neq i} g_{ji}P_j + \nu_i} \ , \tag{14}$$

where ν_i is the noise power and P_i the transmission power on link i.

3.1.1 Information theoretic bound

The most interesting channel model in the performance analysis of ad hoc networks is the well-known Shannon model, which, combined with the BF-resource sharing, yields the best possible insensitive performance in the given network scenario. In theory, the allocations are also Pareto efficient in the sense that no resources that can be used are left unused, cf. previous section and Appendix A.

Shannon capacities give the theoretical limits for the link rates in an AGWN channel of bandwidth W, which depend explicitly on the other active links and noise. In this model the link rates are given by (for a given transmission power configuration τ)

$$v_i(\tau) = W \log_2 (1 + s_i) \ . \tag{15}$$

Although the set of different transmission modes cannot be enumerated as each P_i can have a continuous value between 0 and some maximum transmission power, the spanning rate vectors needed for $\mathbf{R}$ use only the extreme power settings for the links, as noted in Leelahakriengkrai and Agrawal (2003). Figure 1 illustrates this in a two-link case where the links have identical interference impacts on each other. The figure shows the normalized link rates obtained from (15) with different power settings. Clearly, all the non-extremal rates belong to the convex hull spanned by the extremal vectors.

Hence, it is sufficient to consider the transmission modes in which each link is either "off", or "on" with full power. There are thus $2^J - 1$ candidates for the spanning vectors. For these the corresponding link capacities follow directly from (15) and (14).

Note that in this model we have assumed that all the links can be active simultaneously. In practice, hardware and software configurations of the network nodes may invalidate this assumption. For example, it may not be possible to transmit and receive simultaneously or to receive multiple concurrent signals. We will return to this question in Section 3.2 and show how the Shannon model can be combined with physical constraints reducing the number of spanning vectors.

3.1.2 Threshold model, STDMA

In the threshold model, a set of links (which satisfy the possible physical constraints) can operate simultaneously if the signal to noise ratio is adequate at each receiver. In the simplest case, the capacity of link i is constant c_i when s_i exceeds a given threshold t_i and zero otherwise. Such models are often used in the context of Spatial-TDMA (introduced by Nelson and Kleinrock (1985)), where the active links in each time slot must satisfy the above-mentioned condition.

One may distinguish two cases in the threshold model, the ones with and without power control, as e.g. in Johansson and Xiao (2004). In both cases one starts the construction of $\mathbf{R}$ by enumerating all combinations of active links as in the Shannon model. Denote the set of link combinations by L.

If the links use fixed power, $P_i = P_{\max,i}$ for all active links i, $\mathbf{R}$ is constructed as follows. For each, $l \in L$ check whether all $s_i \geq t_i$ when the active links use their respective maximum powers. If the condition holds, the rate vector is included in $\mathbf{R}$.

If power control is assumed, $P_i \in [0, P_{\max,i}]$, nodes can adjust their transmission powers to minimum acceptable levels to avoid causing unnecessary interference (Somarriba (2002)). In this case, for each $l \in L$ check whether there exists a feasible power vector that attains $s_i = t_i$ for all $i \in l$, that is, whether the corresponding set of linear equations has a feasible solution. If the condition holds, the rate vector is included in $\mathbf{R}$.

The model is also easily extended by introducing several thresholds for different rates.

This model can be designed to approximate closely any discrete rate system.

3.2 Modeling MAC with a constraint model

In some scenarios the link activity is constrained by physical limitations or access control protocols. Such constraints can be accounted for using a pairwise link constraint model. In a common MAC-layer model two links can be simultaneously active either with some predefined capacities or not at all. This reflects the situation that the channel is locally reserved for one link among competing transmissions. On the other hand, if the attenuation (power gain) in the SIR formula (14) is very steep as a function of distance, the threshold model can be approximated by the pairwise model.

In the literature, the pairwise link constraint models appear frequently with some differences in how the link constraints are defined. An elementary access model sets the following constraints to the links in the network. A node may not transmit and receive simultaneously and it cannot transmit or receive more than one packet at a time. In other words, all the links connected to a given node belong to different transmission modes. This is often used as an access model with the assumption that other transmissions in the vicinity of the node can operate without conflict using locally distinct frequencies (Hajec and Sasaki (1988); Tassiulas and Sarkar (2002)).

A more detailed MAC model would entail that no two links can be simultaneously active if either of the receiving ends is interfered by the other transmission. In the model presented in Arikan (1984); Nelson and Kleinrock (1985) a transmission can prevent reception everywhere within the transmission range, whereas in the widely applied protocol model by Gupta and Kumar (2000) the interference depends on the locations of the transmitting node so that the closest (with a selected margin) transmission can be successfully received.

3.2.1 Obtaining the rate vectors in the constraint model

Assume that the constraints are defined for link pairs only. Such pairwise constraints can conveniently be handled using a link graph, cf. the flow contention graphs in Huang and Bensaou (2001); Luo et al. (2000) or the compatibility matrix in Nelson and Kleinrock (1985).

Given a network and a set of flows with their routes, the corresponding link graph is constructed as follows: each directed link in the network (that is in use in the scenario) is mapped to a vertex and an edge connects two link graph vertices if the corresponding links cannot be active simultaneously. Conversely, an independent set on the link graph corresponds to a set of links that can be active simultaneously. Thus, the feasible transmission modes are obtained by enumerating the independent sets of the link graph and the corresponding rate vectors $\mathcal{R}$ result from associating the pre-defined capacities to the links in the independent sets. See Figure 2 for an example of a link graph.

This model can also be used in conjunction with the power control models to eliminate the infeasible parameter configurations. To generate the rate vectors in this hybrid case, one reduces the set of all combinations of active links into the set of feasible combinations of active links (where e.g. active links do not share a node) by stating the feasibility constraints in the link graph and enumerating the independent sets. Then the corresponding link rates are determined using the SIR-based models.

Specialized computational methods to utilize the pairwise property in the performance analysis of ad hoc networks are presented in Penttinen and Virtamo (2004).

4 General recursive algorithm for the balance function

In Section 2.2 we defined the recursion step as an LP-problem. Since the state space is often large, it is essential that the computations to solve the problem can be carried out efficiently. In this section we present an efficient computational algorithm for the recursion.

4.1 Reduction of the rate matrix

While the full convex hull $H(\mathcal{R})$ explicitly defines all the available rates and enables simple intuitive definitions, it often contains a lot of redundant information for the computational purposes. Without loss of generality we may reduce $\mathbf{R}$ to contain only rate vectors that are maximal, i.e. including a rate vector $\mathbf{r}_i$ only if $\nexists\, \mathbf{r}_j$, $j \neq i$, such that $\mathbf{r}_j \geq \mathbf{r}_i$. We denote this reduced matrix by $\mathbf{R}'$.

As an extreme example, in a fixed network $\mathbf{R}'$ contains only a single rate vector consisting of the fixed link rates, whereas the corresponding $\mathbf{R}$ spans a J-dimensional hypercube, i.e. it contains all the $2^J - 1$ combinations of active links. Naturally, for this case the balance function is simply defined by (2) and no LP-formulations are needed.

Next we describe our algorithm for this reduced matrix.

4.2 Integrated solution to the recursion

For the reduced matrix $\mathbf{R}'$ we write the recursion step as

$$\begin{aligned} \Phi(\mathbf{x}) &= \min_{\mathbf{q}} \mathbf{e}^{\mathrm{T}}\mathbf{q} \ , \\ \mathbf{R}'\mathbf{q} &\geq \mathbf{b}(\mathbf{x}) \ , \\ \mathbf{q} &\geq \mathbf{0} \ , \end{aligned} \tag{16}$$

which differs from (11) only by the rate constraints.

The important observation is that only the right hand side of the constraints $\mathbf{b}(\mathbf{x})$ depends on the state. Therefore, we are inclined to apply the LP-duality to devise an efficient computational method to solve the balance function.

The dual problem of (16) is given by

$$\begin{aligned} \Phi(\mathbf{x}) = \max_{\mathbf{y}} \mathbf{b}(\mathbf{x})^{\mathrm{T}}\mathbf{y} \ , \\ \mathbf{R'}^{\mathrm{T}}\mathbf{y} \leq \mathbf{e}^{\mathrm{T}} \ , \\ \mathbf{y} \geq 0 \ . \end{aligned} \tag{17}$$

The dual problem has the same optimum value as (16) (Bazaraa et al. (1993)), but the advantage here is that the constraints do not depend on $\mathbf{x}$. Hence, an optimal solution $\mathbf{y}^*$ to the problem in state $\mathbf{x}$ is also a feasible solution for the dual problem in any other state $\mathbf{x}'$.

This leads us to propose integrating the recursion and the solution of the LP-problem into a single problem. The idea of the approach is to calculate the new value of the balance function in the recursion by using a stored solution of (17) in some previously calculated state. If the solution is not optimal, we can update it by the standard simplex iterations (cf. e.g. Bazaraa et al. (1993)) until the optimum is found.

Compared to the standard simplex method applied to the primal problem (16), this approach has two significant advantages.

- We need to find only one starting feasible solution for the whole recursion. In contrast, solving the LP-problem by standard means would first require finding a feasible starting solution at each state.

- Given that the iteration is started from the optimal solution for a state which is close (possibly adjacent) to the current one, the simplex iteration converges in a few steps to the optimum. The number of iterations the simplex would require to converge to the optimum from a arbitrary feasible solution could be large.

Although the algorithm can be elegantly described using the simplex and the dual problem, it is often more efficient to apply the dual simplex algorithm (Taha (1997)) directly to

the primal problem (16), which is then supplemented with slack variables (or in case full $\mathbf{R}$ is used, one may use (11)).

In the dual simplex algorithm we store the optimal bases (sets of rate vectors defining the solution) of the primal solutions instead of the solutions themselves. By duality, the bases satisfy optimality conditions but are not necessarily feasible. The intuition behind the dual simplex iteration can be explained by looking at the formulation (11). $\mathbf{R}$ spans the convex hull of attainable rates and we are looking for the intersection of the surface of hull and the line going from origin to the direction of $\mathbf{b}(\mathbf{x})$. Each basis of the solution to (11) defines a facet of the convex hull. A dual simplex iteration first checks whether the current basis is feasible (and thus optimal), i.e. whether the facet is penetrated by the direction $\mathbf{b}(\mathbf{x})$, and if not, replaces one of the rate vectors in the basis by another thus defining a neighboring facet. Thus the algorithm searches the intersection point by "crawling" towards the point facet by facet on the surface of the convex hull.

4.3 Computational aspects

The performance of the algorithm can further be increased by three off-line preparations, removal of non-spanning vectors from $\mathbf{R}$, reduction of $\mathbf{R}$ and by choosing the suitable formulation from (11), (16) or their dual problems with a suitable simplex algorithm.

The relative computational efficiency of different formulations depends on the number of variables in the problem setting. Let m and m' be the number of spanning rate vectors without and with the reduction, respectively. Whereas formulation (11) using $\mathbf{R}$ has m variables, (16) with $\mathbf{R}'$ has $m' + J$ variables.

The simplex iteration step in the dual problem (17) consists of taking the matrix inverse of a $m \times m$ matrix (or $m' \times m'$) and then evaluating J variables for the entering variable. Using the dual simplex we take the inverse of $J \times J$ matrix and then evaluate m (or m') variables for entering variable.

Our implementation of the algorithm is written in Mathematica. The LP-problem is

solved using a built-in LP-solver in states $\mathbf{x} \leq \mathbf{1}$ and for the rest using a dual simplex-implementation. In these cases the starting basis is chosen to be the basis from the previous state along the axis $d = \arg\max_i \mathbf{x}$. Example 3 in Section 5.3 discusses a case where LP-solutions need to be used.

The proposed algorithm outperforms the alternative of using an LP-solver package to evaluate (16) directly in each state. In Example 3, a Mathematica implementation of the algorithm was nearly 4 times as fast as Mathematica's built-in LP-solver, despite the fact that the solver uses an optimized internal code.

The discussion above dealt with the numbers of links and spanning rate vectors. In a broader perspective these are of minor concern as the state-space explosion limits severely the number of flow classes that can be considered in any computational scenario. However, whereas in an ordinary Markov-system one finds the equilibrium distribution by inverting a square matrix the size of which equals to the number of states, here it suffices to go through the states only once. Thus the complexity increases linearly, as opposed to quadratically, as the number of considered states increases. The obtained advantage is considerable and allows much larger systems to be analyzed.

5 Examples

In this section we explicitly illustrate some details of the ideas discussed in the article. First, we shed light on the concept of extended balanced fairness in a simple case where two links cannot access the channel simultaneously. The second example brings forth the idea of the convex hull of the achievable link rates and the third merely considers a case where the algorithm described in Section 4 can be used for computational efficiency. Finally, we illustrate the effect of one more degree of freedom by considering how throughput is affected by two different routing schemes.

5.1 Example 1: Extended balanced fairness

The system consists of three nodes (A,B,C) and two radio links (1,2), with capacities c_1 and c_2. Node A cannot reach node C directly. There are two flow classes: class-1 flows from B to C utilize link 1 only while class-2 flows from A to C use both link 1 and link 2. Figure 3 illustrates the system.

Assume that both links cannot be used at the same time as node B cannot transmit and receive simultaneously. The virtual network $\upsilon \in \Upsilon$ is now defined by a single parameter t, the schedule, defining which portion of time is scheduled for link 1. For simplicity, we consider the normalized effective link capacities which are thus,

$$c_1(t) = t \ , \qquad c_2(t) = \sigma(1-t) \ ,$$

where $\sigma = c_2/c_1$ is the relative capacity of link 2. In the link capacity space this model defines the available virtual networks as the convex hull spanned by the vectors (1,0) and (0,σ), see Figure 4.

From the figure we obtain directly the constraining equation for the link rates (cf. eq. (12))

$$\underbrace{\begin{pmatrix} 1 & \frac{1}{\sigma} \end{pmatrix}}_{\mathbf{D}} \begin{pmatrix} r_1 \\ r_2 \end{pmatrix} \leq \underbrace{1}_{\mathbf{d}} \ .$$

The balance function is now defined by (13) yielding

$$\Phi(x) = \underbrace{\frac{1}{1}}_{\mathbf{d}} \underbrace{\begin{pmatrix} 1 & \frac{1}{\sigma} \end{pmatrix}}_{\mathbf{D}} \underbrace{\begin{pmatrix} 1 & 1 \\ 0 & 1 \end{pmatrix} \begin{pmatrix} \Phi(x-e_1) \\ \Phi(x-e_2) \end{pmatrix}}_{\mathbf{b(x)}} = \Phi(x-e_1) + (1+\frac{1}{\sigma})\,\Phi(x-e_2) \ .$$

This recursion is solved by the balance function

$$\Phi(\mathbf{x}) = \binom{x_1+x_2}{x_1} (1+\frac{1}{\sigma})^{x_2} \ . \tag{18}$$

The bandwidth allocations to the classes (relative to c_1) are thus by (1),

$$\begin{cases} \phi_1(x) &= \dfrac{x_1}{x_1+x_2} \ , \\ \phi_2(x) &= \dfrac{x_2}{(1+\frac{1}{\sigma})(x_1+x_2)} \ . \end{cases}$$

The normalization constant can be easily calculated,

$$G(\boldsymbol{\rho}) = \frac{1}{1-\rho_1-(1+\frac{1}{\sigma})\rho_2} \ ,$$

from which one readily obtains the throughputs using (6),

$$\gamma_1 = 1-\rho_1-(1+\frac{1}{\sigma})\rho_2 \ , \quad \gamma_2 = \frac{1-\rho_1}{(1+\frac{1}{\sigma})} - \rho_2 \ . \tag{19}$$

5.2 Example 2: Interference constrained link rates

Consider a symmetric case with two identical links with unit nominal capacity, see Figure 5. When both links are operated simultaneously, they receive a reduced capacity $\mathbf{c}_{11} = (\frac{1}{1+\alpha}, \frac{1}{1+\alpha})$, because of the mutual interference, the strength of which is described by the parameter α. We assume now that $\alpha < 1$, whence $\mathbf{c}_{11}$ is also active in spanning the convex hull of the available rates, see Fig. 6: Otherwise, the hull is spanned by $\mathbf{c}_{10}$ and $\mathbf{c}_{01}$ only and the problem is essentially the same as the one already covered in 5.1.

In the BF recursion, the ratios of the bandwidth allocations $\phi_i(\mathbf{x})$ in a state $\mathbf{x}$ are fixed,

$$\phi_i(\mathbf{x}) \sim \Phi(\mathbf{x}-\mathbf{e}_i), \quad i=1,2 \ . \tag{20}$$

Without loss of generality, assume $x_1 \geq x_2$. In our symmetric system this implies that $\phi_1(\mathbf{x}) \geq \phi_2(\mathbf{x})$. The largest allocations are determined in the $\mathbf{c}$-plane by the intersection of the line through the origin with slope $\Phi(\mathbf{x}-\mathbf{e}_2)/\Phi(\mathbf{x}-\mathbf{e}_1)$ and the line going through $\mathbf{c}_{10}$

and $\mathbf{c}_{11}$ as depicted in Figure 6.

By a simple calculation we get

$$\phi_1(\mathbf{x}) = \frac{\Phi(\mathbf{x}-\mathbf{e}_1)}{\Phi(\mathbf{x}-\mathbf{e}_1)+\alpha\,\Phi(\mathbf{x}-\mathbf{e}_2)}, \quad \phi_2(\mathbf{x}) = \frac{\Phi(\mathbf{x}-\mathbf{e}_2)}{\Phi(\mathbf{x}-\mathbf{e}_1)+\alpha\,\Phi(\mathbf{x}-\mathbf{e}_2)} \ , \tag{21}$$

which by $\Phi(\mathbf{x}) = \Phi(\mathbf{x}-\mathbf{e}_i)/\phi_i(\mathbf{x})$ leads to the recursion

$$\Phi(\mathbf{x}) = \begin{cases} \Phi(\mathbf{x}-\mathbf{e}_1)+\alpha\,\Phi(\mathbf{x}-\mathbf{e}_2), & \text{for } x_1 \geq x_2 \ , \\ \\ \alpha\,\Phi(\mathbf{x}-\mathbf{e}_1)+\Phi(\mathbf{x}-\mathbf{e}_2), & \text{for } x_1 \leq x_2 \ . \end{cases} \tag{22}$$

Denoting $a = \min(x_1, x_2)$ and $b = \max(x_1, x_2)$, the solution to the recursion can be written as

$$\Phi(a,b) = \sum_{i=0}^{a} \binom{b-1+a-i}{a-i} \frac{b-a+i}{b} \alpha^{a-i}(1+\alpha)^i \ . \tag{23}$$

The proof that (23) indeed solves (22) is given in Appendix C. Generally one has to evaluate the balance function numerically; even in this simple scenario the explicit form of the balance function was difficult to obtain. For the numerical evaluation of the value of $\mathrm{E}[x_i]$, the recursive expression (22) is more efficient than (23).

5.3 Example 3: Numerical recursion

We demonstrate the use of the scheme proposed in Section 4 in the following numerical scenario with three traffic classes. The network consists of six nodes which operate on a single channel. The access point (AP) is able to receive all incoming links simultaneously, but the links are assumed to interfere with each other. The node locations are given by (in 1000 m) AP $(0,0)$, A $(-2.6,0)$, B $(2,0)$, C $(4.4,0)$, D $(5,1.6)$, E $(6,-1)$. The scenario is illustrated in Figure 7.

The channel capacity is assumed to follow the Shannon model (see Section 3), with the parameters described in Appendix D. Further, all the nodes except for the access point

cannot transmit and receive simultaneously, and no more than one packet at a time. The matrix $\mathbf{R}$ consists of rate vectors calculated using the Shannon model for the transmission modes shown in Figure 8.

Numerical computation was done using the formulation (11) with dual simplex iterations. Figure 9 shows the throughputs experienced by the classes as the load of class 1 is increased. Class-2 throughput is the lowest due to the weak link D $\rightarrow$ B. The sharp decline in class-2 and class-3 throughput at high class-1 load is caused by the resource sharing; if the rate allocated to class-1 is greater than the transmission mode 6 (cf. Figure 8) can provide, one uses mode 2 to a greater extent, which makes the link from node B to access point the bottleneck for the other two classes.

5.4 Example 4: A routing example

Routing is an additional degree of freedom that can be utilized in multi-hop networks. We have not addressed the issue elsewhere in this article, but illustrate the concept here by a simple example.

Consider the first two examples as routing scenarios. Now the three nodes are parallel and node C is a base station. We wish to determine the throughput experienced by class-1 user at node B in the routing scenarios where either class-2 connects to the base station directly or class-2 traffic is relayed through node B. In other words, is it advantageous for B to participate in the network operation by relaying the packets of A?

The numerical parameters of the example are described in Appendix D. Node B is at the distance 2000 m from the base station and node A is located behind node B at the distance d, see Figure 10 for illustration.

Case 1, where node B retransmits the packets of A corresponds to Example 1 with $\alpha = c_1/c_2$, where c_i are given by (15). Case 2, where node A communicates directly with the base station is closely related to Example 2 but now the links are not symmetric. However, reasoning similar to that illustrated in Figure 6 can be applied in the convex hull to construct

the recursion

$$\Phi(\mathbf{x}) = \begin{cases} \frac{1}{c_2^{(01)} c_1^{(11)}} ((c_2^{(01)} - c_2^{(11)})\Phi(\mathbf{x} - \mathbf{e}_1) + c_1^{(11)}\Phi(\mathbf{x} - \mathbf{e}_2)) \ , \\ \frac{1}{c_1^{(10)} c_2^{(11)}} (c_2^{(11)}\Phi(\mathbf{x} - \mathbf{e}_1) + (c_1^{(10)} - c_1^{(11)})\Phi(\mathbf{x} - \mathbf{e}_2)) \ , \end{cases}$$

which can be used to evaluate the steady state distribution by (4) to approximate throughput. Again, the capacities are determined by the Shannon model.

Figure 11 shows the class-1 (traffic of node B) throughput for the routing scenarios as a function of the distance d between nodes A and B. The traffic load is 915 Kbits/s for both classes. From the results we see that by forcing the bandwidth sharing to be fair we promote co-operation as the channel becomes worse for A. On the other hand, significant gains in throughput can be obtained in fair multirate systems by routing. A more detailed elaboration of the topic is left for future work.

6 Conclusions

This paper studied flow-level dynamics of ad hoc networks and illustrated how the concept of balanced fairness can be extended to allow the derivation of insensitive performance measures of a wireless multi-hop network under elastic traffic in a dynamic setting.

We adapted the balanced fairness analysis tools to a general modeling framework in which the wireless network resources are subject to linear constraints. The resource model allows several degrees of freedom to be incorporated in the analysis. In particular, we discussed how power control and MAC-layer reservation protocols affect the link capacities and how these can be described by the resource model.

Finally, we presented an efficient computational algorithm for the performance analysis in this general setting. The proposed LP-formulations of the original recursion step problem restrict the state dependency to the right hand side of the constraints. This allows applying LP-duality to devise a method in which previous solutions can be utilized to integrate the

solution of the LP-problem with the balance function recursion. Accordingly, at the expense of some storage space, we can now reach the optimum at each recursion step with few or no iterations at all.

The analysis is still limited to scenarios where the number of flow classes is rather small as the state space grows exponentially with the number of flow classes. However, the presented methods significantly expand the reach of mathematical analysis in comparison to conventional Markov models. Under balanced fairness the computational effort is linear with respect to the number of states (as opposed to quadratic) and the proposed linear programming scheme for the resource model considerably reduces the effort required per state.

Tobagi (1987) concluded that due to the complexity of the issue there are basically two analytical approaches in modeling the performance of multihop radio networks. In addition to the explicit results on small networks, the topic of the present article, one may attempt to provide approximations based on major simplifying system assumptions. This alternative remains open for further study.

Acknowledgements

This work has been partially funded by Finnish Defence Forces Technical Research Center and the Academy of Finland (GETA and Grant decision number 202204). Riku Jäntti would like to acknowledge financial support from the Academy of Finland (Grant decision number 10222).

Appendix

A Validity of LP-formulation and Pareto efficiency

Consider a spanning rate vector $\mathbf{r}$ associated to the convex hull $H(\mathcal{R})$ and define the axis projections of the vector as the subsets of $\mathbf{x}$ where $1, ..., J$ components are replaced with zero. Projection to direction i means thus $\mathbf{x}$ with x_i replaced with zero.

Consider then the following two conditions:

I All axis projections of a point in the convex hull belong to the convex hull.

II All axis projections of a point in the convex hull belong to the interior of the convex hull.

Condition I equals to coordinate convexity, see Aein (1978).

Lemma 1 *If all the spanning rate vectors satisfy condition I or II then any point of the hull satisfies the same condition.*

Proof for condition I. Let $\mathbf{r}_1, ..., \mathbf{r}_n$ be the spanning vectors and let $\mathbf{x}$ be a point in the convex hull; $\mathbf{x} = p_1\mathbf{r}_1 + ... + p_n\mathbf{r}_n$ for some $\mathbf{p}$, $\mathbf{e}^{\mathrm{T}}\mathbf{p} \leq 1$. Consider the projection of $\mathbf{x}$ along the axis i, which can be written using the projections of the spanning vectors along the axis i as $\mathbf{x}' = p_1\mathbf{r}'_1 + ... + p_n\mathbf{r}'_n$.

Since the projections $\mathbf{r}'_j \ \forall j$ belong to the convex hull and $\mathbf{e}^{\mathrm{T}}\mathbf{p} \leq 1$ also $\mathbf{x}'$ belongs to the convex hull. For condition II a similar reasoning applies. □

Lemma 2 *If condition I holds for the spanning rate vectors, the recursion step for balance function is given by (11).*

Proof. The actual rate constraints for the problem are of the form $\mathbf{Rq} \geq \mathbf{b}$. We show that under condition I there exists an optimum solution $\mathbf{q}^{**}$ for which the rate constraints are met with equality.

Assume that the equality does not hold, i.e., at the optimum there exists i such that the i:th component of $\mathbf{r} = \mathbf{R}\mathbf{q}^*$, where $\mathbf{q}^*$ is a vector realizing the optimum, is strictly larger than b_i. Thus $r_i = b_i + \delta$ for some $\delta > 0$.

Let $\mathbf{r}'$ be the projection of $\mathbf{r}$ along the axis i; $\mathbf{r}'$ is equal to $\mathbf{r}$ but with a zero as the i:th element. From condition I we get that the $\mathbf{r}'$ belongs to the convex hull spanned by $\mathbf{R}$ and scaled by $(\mathbf{e}^{\mathrm{T}}\mathbf{q}^*)$. Then, $\exists\, \mathbf{q}'$ such that $\mathbf{R}\mathbf{q}' = \mathbf{r}'$ with $\mathbf{e}^{\mathrm{T}}\mathbf{q}' \leq \mathbf{e}^{\mathrm{T}}\mathbf{q}^*$.

Next we construct a new solution to the problem. Let $\mathbf{q}^{**} = (1-x)\mathbf{q}' + x\mathbf{q}^*$, where $x = b_i/(b_i+\delta)$. Now $\mathbf{R}\mathbf{q}^{**} = (1-x)\mathbf{r}' + x\mathbf{r}$ for which the i:th component is $(1-x)\cdot 0 + x\cdot(b_i+\delta) = b_i$, otherwise it is identical to $\mathbf{r}$ and $\mathbf{r}'$.

The value of the objective function for this new solution is $\mathbf{e}^{\mathrm{T}}\mathbf{q}^{**} = (1-x)(\mathbf{e}^{\mathrm{T}}\mathbf{q}') + x(\mathbf{e}^{\mathrm{T}}\mathbf{q}^*) \leq \mathbf{e}^{\mathrm{T}}\mathbf{q}^*$, since $\mathbf{e}^{\mathrm{T}}\mathbf{q}' \leq \mathbf{e}^{\mathrm{T}}\mathbf{q}^*$. Strict inequality would contradict with the assumption that $\mathbf{q}^*$ is optimal and therefore the two values of objective function must be equal. Thus, $\mathbf{q}^{**}$ is also an optimal solution to (11), but with i:th constraint met with equality. The same reasoning can be repeated to construct a solution for which all constraints are met as equalities. □

Lemma 3 *If condition II holds, the optimum solution to (11) is Pareto efficient in resource usage so that there is no free capacity left in system.*

Proof. We show that under the condition II there does not exist any optimal solution, for which there is free capacity left on some link.

The proof follows closely the previous case. The only difference is that now the projection $\mathbf{r}'$ lies in the interior of the scaled convex hull and thus $\exists\, \mathbf{q}'$ such that $\mathbf{R}\mathbf{q}' = \mathbf{r}'$ with $\mathbf{e}^{\mathrm{T}}\mathbf{q}' < \mathbf{e}^{\mathrm{T}}\mathbf{q}^*$. Now we can again generate the new solution in the hull, $\mathbf{q}^{**}$, as in the previous proof. However, the corresponding solution $\mathbf{q}^{**}$ has an objective function value that is strictly less than $\mathbf{e}^{\mathrm{T}}\mathbf{q}^*$. This contradicts with the assumption that $\mathbf{q}^*$ is optimal.

Whereas in Lemma 1 we showed that under condition I there always exists an optimal solution for which the constraints are met as equality, in this case the solution cannot be

optimal unless the constraints are met as equality. Hence, at the optimum, there cannot be $\delta > 0$ free capacity on any link i. $\square$

Condition II holds only if all the links are interdependent so that an increase in a link rate automatically means a decrease in all the other rates. This happens, for example, in the Shannon model. However, condition II is only of theoretical interest. In large networks, the interaction between distant links is so weak that they are practically independent.

B Redundancy of non-spanning vectors

Property 1 *Only vectors* $\mathbf{r}_i \in \mathbf{R}$ *which reside on the surface of convex hull of available link rates can exist in an optimal solution to (11).*

Proof:

A non-spanning column vector of $\mathbf{R}$ can be expressed using the spanning vectors and suitable coefficients, i.e. $\mathbf{r}_x = \sum \mathbf{r}_i x_i$, $\sum x_i < 1$. Assume now that $\mathbf{r}_x$ belongs to the optimal basis. Then there exists a vector of dual variables, $\mathbf{y}$, for which (complementary slackness, Bazaraa et al. (1993)) $\mathbf{r}_x^{\mathrm{T}}\mathbf{y} = 1$ and (dual feasibility, Bazaraa et al. (1993)) $\mathbf{r}_i^{\mathrm{T}}\mathbf{y} \leq 1$, $\forall i$. Now $\mathbf{r}_x^{\mathrm{T}}\mathbf{y} = \sum(\mathbf{r}_i x_i)^{\mathrm{T}}\mathbf{y} = \sum(\mathbf{r}_i^{\mathrm{T}}\mathbf{y})x_i \leq \sum x_i < 1$, which is a contradiction. $\square$

C Proof for Example 5.2

Denoting $a = \min(x_1, x_2)$ and $b = \max(x_1, x_2)$, the recursion can be written as

$$\Phi(a, b) = \alpha\Phi(a-1, b) + \Phi(a, b-1) \ ,$$

which is solved by the expression (23).

Proof:

$$
\begin{aligned}
&\alpha\Phi(a-1,b)+\Phi(a,b-1)= \\
&=\sum_{i=0}^{a-1}\binom{b-2+a-i}{a-1-i}\frac{b-a+1+i}{b}\alpha^{a-i}(1+\alpha)^i \\
&\quad+\sum_{i=0}^{a}\binom{b-2+a-i}{a-i}\frac{b-1-a+i}{b-1}\alpha^{a-i}(1+\alpha)^i \\
&=\sum_{i=0}^{a-1}\left\{\binom{b-2+a-i}{a-1-i}\frac{b-a+1+i}{b}\right. \\
&\quad\left.+\binom{b-2+a-i}{a-i}\frac{b-1-a+i}{b-1}\right\}\alpha^{a-i}(1+\alpha)^i+(1+\alpha)^a \\
&=\sum_{i=0}^{a-1}\left\{\binom{b-2+a-i}{a-1-i}\left(\frac{b-a+1+i}{b}+\frac{b-1-a+i}{a-i}\right)\right\}\alpha^{a-i}(1+\alpha)^i+(1+\alpha)^a \\
&=\sum_{i=0}^{a-1}\binom{b-1+a-i}{a-i}\frac{b-a+i}{b}\alpha^{a-i}(1+\alpha)^i+(1+\alpha)^a \\
&=\sum_{i=0}^{a}\binom{b-1+a-i}{a-i}\frac{b-a+i}{b}\alpha^{a-i}(1+\alpha)^i=\Phi(a,b)\ \square.
\end{aligned}
$$

D Simulation parameters

Capacity of link i according to the Shannon model is given by,

$$
c_i = W\log_2\left(1+\frac{g_{ii}p_i}{\sum_{j\neq i}g_{ji}p_j+\nu_i}\right)\ , \tag{24}
$$

where g_{ij} is $d_{ij}^{-\alpha}$, d being the distance between the transmitter of link i and the receiver of link j. In the numerical examples we have taken

$$
\begin{cases}
W &= 3.84\,\text{MHz}, \\
\alpha &= 4, \\
\nu_i &= 1.5287\cdot 10^{-11}\,\text{mW}, \\
p_i &= 125\,\text{mW}.
\end{cases} \tag{25}
$$

References

Aein, J. (1978). A multi user, blocked-calls-cleared, demand access model. *IEEE Transactions on Communications 26*(3).

Arikan, E. (1984). Some complexity results about packet radio networks. *IEEE Transactions on Information Theory IT-30*(4), 681–685.

Bazaraa, M., H. Sherali, and C. Shetty (1993). *Nonlinear programming; theory and algorithms*. Wiley.

Bonald, T. and A. Proutière (2002). Insensitivity in processor-sharing networks. *Performance Evaluation 49*, 193–209.

Bonald, T. and A. Proutière (2003). Insensitive bandwidth sharing in data networks. *Queuing Systems 44*, 69–100.

Bonald, T. and A. Proutière (2004). On performance bounds for balanced fairness. *Performance Evaluation 55*, 25–50.

Bonald, T., A. Proutière, J. Roberts, and J. Virtamo (2003). Computational aspects of balanced fairness. In Charzinski and et al. (Eds.), *Providing Quality of Service in Heterogeneous Environments*, pp. 801–810. Elsevier Science.

Gupta, P. and P. R. Kumar (2000). The capacity of wireless networks. *IEEE Transactions on Information Theory 46*(2), 388–404.

Hajec, B. and G. Sasaki (1988). Link scheduling in polynomial time. *IEEE Transactions on Information Theory 34*(5), 910–917.

Huang, X. and B. Bensaou (2001). On max-min fairness and scheduling in wireless ad hoc networks: analytical framework and implementation. In *Proc. ACM MobiHOC 2001*, pp. 221–231.

Johansson, M. and L. Xiao (2004). Scheduling, routing and power allocation for fairness in wireless networks. In *Proc. IEEE Vehicular Technology Conference*.

Leelahakriengkrai, R. and R. Agrawal (2003). Scheduling in multimedia CDMA wireless networks. *IEEE Transactions on Vehicular Technology 52*(1).

Luo, H., S. Lu, and V. Bharghavan (2000). A new model for packet scheduling in multihop wireless networks. In *Proc. ACM MOBICOM 2000*, pp. 76–86.

Massoulié, L. and J. Roberts (2002). Bandwidth sharing: Objectives and algorithms. *IEEE/ACM Transactions on Networking 10*(3), 320–328.

Mo, J. and J. Walrand (2000). Fair end-to-end window-based congestion control. *IEEE/ACM Transactions on Networking 8*(5), 556–567.

Nelson, R. and L. Kleinrock (1985). Spatial tdma: A collision-free multihop channel access protocol. *IEEE Transactions on Communications 33*(9), 934–944.

Penttinen, A. and J. Virtamo (2004). Performance of wireless ad hoc networks under balanced fairness. In *Proceedings of Networking 2004*, pp. 235 – 246.

Somarriba, O. (2002). On constraint power control for spatial tdma in multi-hop ad hoc radio networks. In *Proceedings of the 2nd Swedish Workshop on Wireless Ad-hoc Networks*, Stockholm, Johannesbergs Slott.

Taha, H. (1997). *Operations research, an introduction* (6th ed.). Prentice Hall.

Tassiulas, L. and S. Sarkar (2002). Maxmin fair scheduling in wireless networks. In *Proc. IEEE INFOCOM 2002*, pp. 764–772.

Timonen, V. (2003). Simulation studies on performance of balanced fairness. Master's thesis, Helsinki University of Technology. `http://www.netlab.hut.fi/tutkimus/fit/publ/thesis_Timonen.pdf`.

Tobagi, F. A. (1987). Modeling and performance analysis of multihop packet radio networks. *Proceedings of the IEEE 75*(1), 135–155.

Footnotes

(Section 2.2.2) [1]Coordinate convexity means that if we take any vector from the convex hull and replace any number of its components by zero, the resulting vector still belongs to the hull $\{\mathbf{Rp} \mid \mathbf{e}^{\mathrm{T}}\mathbf{p} \leq 1, \mathbf{p} \geq \mathbf{0}\}$.

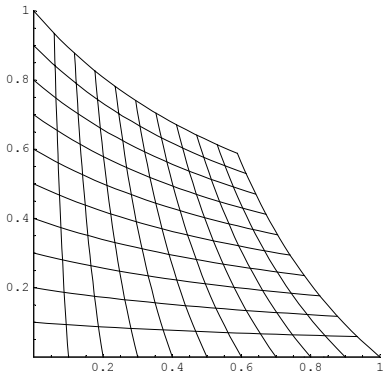

Figure 1: Normalized link rates of two identical links obtained through power control.

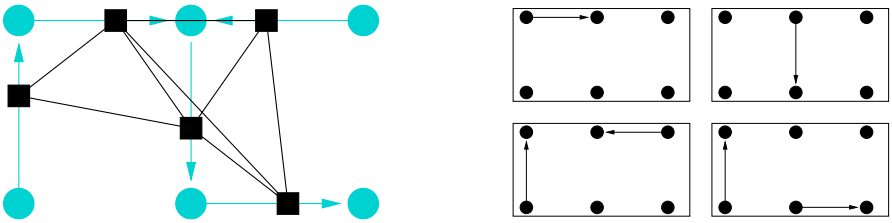

Figure 2: An example of link graph and its independent sets. In this example, two links cannot be active simultaneously if either of the receiving nodes is within the reach of both transmissions.

Figure 3: Example 1.

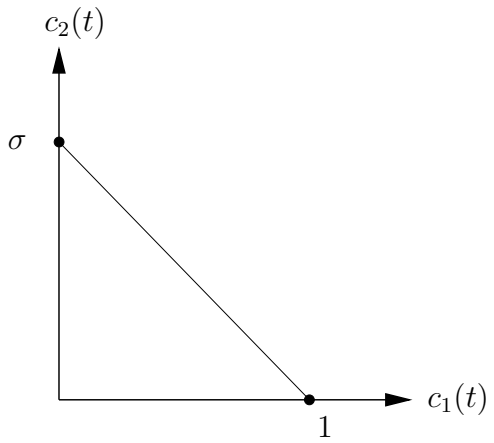

Figure 4: Capacity diagram of Example 1.

Figure 5: Example 2.

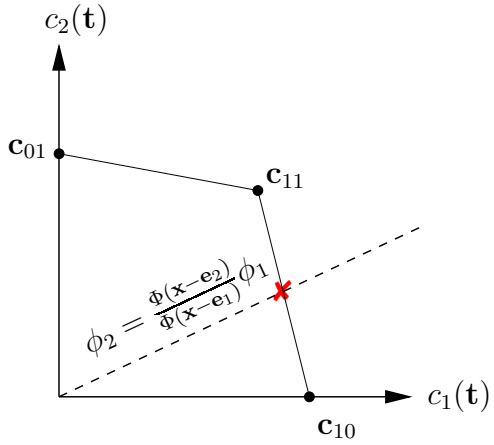

Figure 6: Determining the largest feasible allocation in a direction defined by BF.

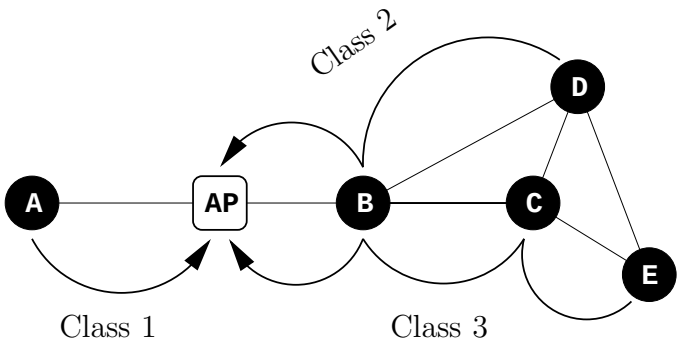

Figure 7: Example 3.

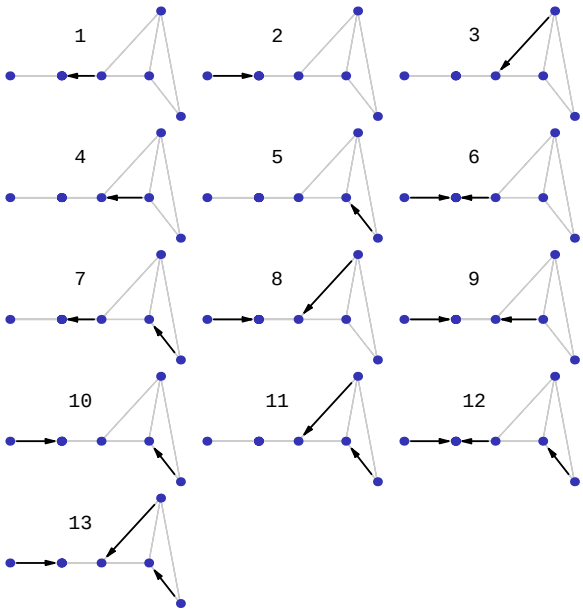

Figure 8: The transmission modes of Ex. 3.

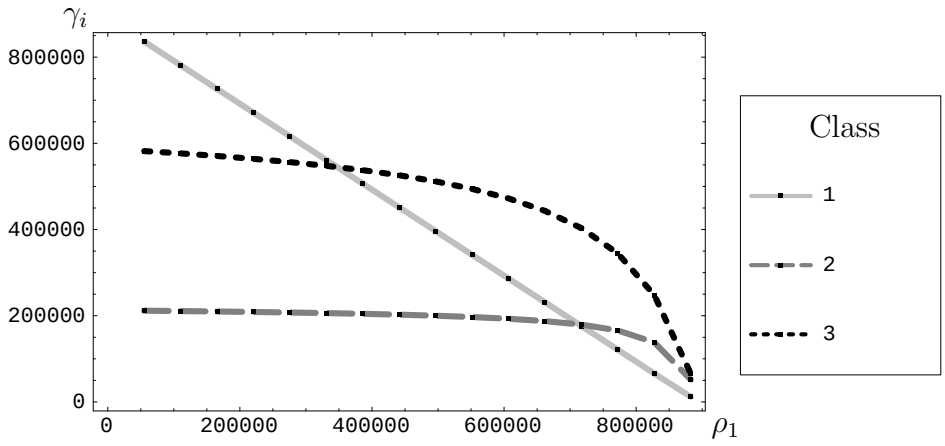

Figure 9: Throughputs in Ex. 3 when $\rho_2 = \rho_3 = 45.7$ Kbits/s.

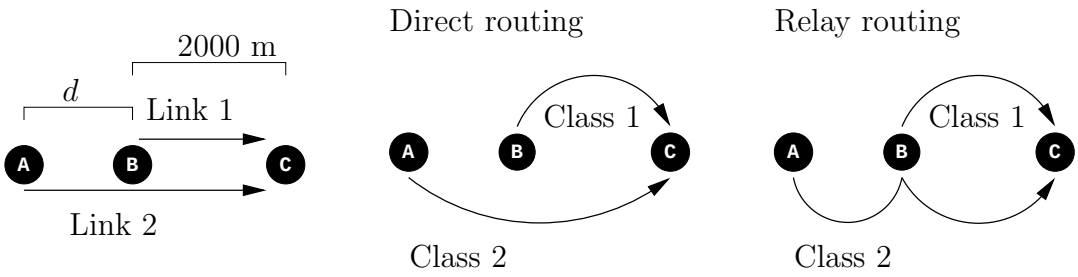

Figure 10: Example 4.

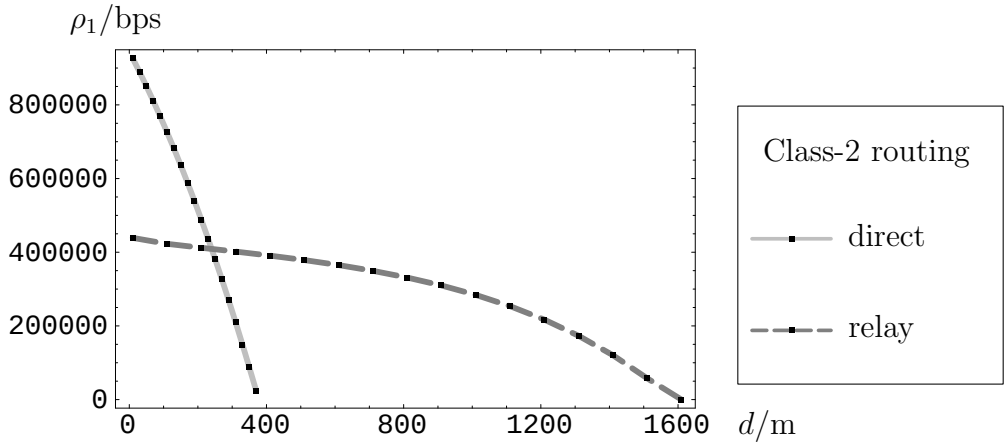

Figure 11: Throughputs of class 1 $\rho_1 = \rho_2 = 915$ Kbits/s for different distances